Influence of H_3PO_4 on the electrochemical behaviour of the PbO_2 electrode

H. Döring* and K. Wiesener

Dresden University of Technology, Department of Chemistry, Mommenstrasse 13, O-8027 Dresden (FRG)

J. Garche

Centre of Solar Energy and Hydrogen Research (Stuttgart and Ulm), Rittinghaus-Strasse 2, W-7913 Senden (FRG)

W. Fischer

Central Institute of Solid State Physics and Material Science, Helmholzstrasse 20, O-8027 Dresden (FRG)

Abstract

Passivation caused by sulfate formation within corrosion layers during cyclic deep discharge of PbO_2 electrodes with grids free of antimony can be diminished by addition of phosphoric acid to the electrolyte. The mechanism was studied by means of cyclovoltammetric and potential-step measurements, X-ray diffraction and scanner electron microscopy (SEM). It was observed that phosphate ions adsorbed specifically on lead dioxide influence nucleation and nuclei growth of PbO_2. During discharge of PbO_2 formed in this manner a $PbSO_4$ of extremely fine grain and dense structure was found, which protects PbO_2 against further discharge and thus prevents an irreversible sulfation of the corrosion layer.

Introduction

Since the beginning of this century a huge number of reports have been given on the addition of H_3PO_4 or phosphates to sulfuric acid electrolytes in lead/acid batteries, e.g. refs. 1–10. Special attention has been paid to the improvement of cyclic life of the positive electrode caused by reduction of shedding and minimizing the formation of refractory sulfate. The charge and discharge current density should be elevated by adding phosphorous compounds. However, adverse effects such as capacity loss [11, 12], poor low temperature performance [13] and increased shedding at the negative electrode [7] have also been reported.

Due to the widespread application of PbCa grids the addition of H_3PO_4 has gained in significance for practical use, since it avoids the formation of insulating layers at deep discharge cycling especially in combination with gelled electrolytes [14–18].

It has been shown that phosphate enters the positive plate during the charging process and leaves it during discharge [19].

---

*Author to whom correspondence should be addressed.

In order to investigate the mechanism effected by phosphoric acid at PbO_2 electrodes, Bullock and McClelland [20] performed systematic tests on corrosion by means of cyclic voltammetry. By electron microprobe analysis Mahato [21] demonstrated the incorporation of phosphorus into the corrosion layer which prevented the formation of an insulating $PbSO_4$ layer.

Applying impedance measurements Carr and Hampson [22] observed a specific adsorption of phosphate ions on α-PbO_2 as well as on β-PbO_2. The existence of soluble lead(IV) species within sulfuric acid containing H_3PO_4 has been proved by several authors [23–27]. The reduction of soluble Pb(IV) species to lead at the negative electrode leads to a moss-like structure that may result in a short circuit of the cell [28].

More recently the effect of H_3PO_4 on the charge and discharge reactions of PbO_2 has been investigated by Hampson and co-workers using cyclic voltammetry and potentiostatic pulses on pure lead as well as on various Pb alloys [29].

In 1988 Voss [28] presented an excellent review of the up-to-date knowledge of the influence of phosphoric acid on the electrochemical behaviour of the lead/acid cell. The literature cited here suggests that the influence of H_3PO_4 is very complex and mainly restricted to the positive electrode. In this paper we hoped to contribute to a better understanding of the effects of phosphoric acid on the mechanism at PbO_2 electrodes.

Experimental

A cylinder of pure lead (99.99%) was embedded in a teflon holder. The electrode surface (exposed area 7.54×10^{-2} cm^2) was mechanically polished under running water on 600 grade silicon carbide paper and washed by distilled water before setting in the cell. The measurements were carried out at 22 °C in H_2SO_4 (0.85 mol/l). Various amounts of H_3PO_4 were added to the electrolyte. All potentials given in this paper refer to an $Hg/Hg_2SO_4/H_2SO_4$ (4.97 M) reference electrode. If not noted otherwise the potentiodynamic measurements (potentiostat PS 4) were carried out at a potential scan rate of 10 mV/s which was suitable for the investigation of smooth electrodes, although very high from the practical point of view with respect to utilization, passivation and crystal sizes of a porous electrode. Electron microscope measurements were carried out on a SEM type TESLA BS 340 instrument, and for electron microprobe analyses the system SEMQ/KEVEX 5100 was used.

Results and discussion

As we could perceive from previous cyclovoltammetric tests, the addition of H_3PO_4 has no essential influence on the cyclovoltammetric behaviour of the lead electrode within the potential range -1600 to -500 mV upto a phosphoric acid concentration of 7×10^{-2} mol/l. Therefore further cyclic measurements were performed within the potential range of $+300$ to $+1600$ mV only.

Figure 1 shows the cyclovoltammograms of the $PbO_2/PbSO_4$ electrode at the 90th cycle in H_2SO_4 (0.85 M) at various phosphoric acid concentrations. Increasing addition of phosphoric acid evidently effects an anodic shift of the oxidation peaks (α- and β-PbO_2, O_2 evolution) accompanied by a simultaneous decrease of peak area excepted at a H_3PO_4 concentration of 10^{-2} mol/l where the peak was increased. On increasing
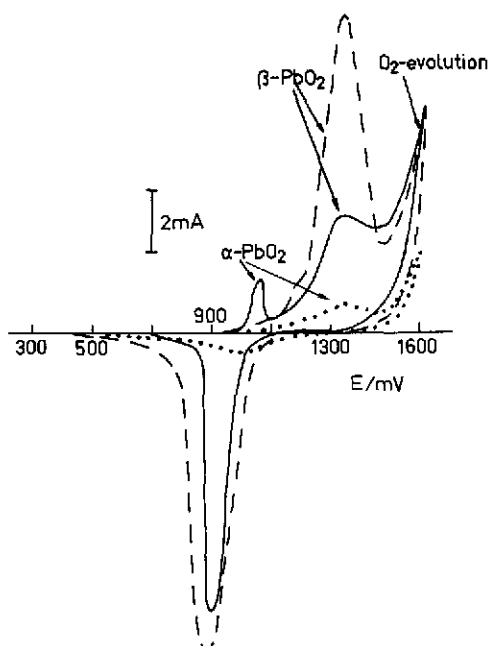
Fig. 1. Cyclovoltammograms of $PbO_2/PbSO_4$ electrodes at the 90th cycle in 0.85 M H_2SO_4 in dependence on the H_3PO_4 added: —— 0 mol/l, – – – 10^{-2} mol/l, · · · · · 7×10^{-2} mol/l.

the H_3PO_4 concentration the α-PbO_2 peak seems to disappear completely, however, cyclovoltammetric measurements performed under continuous addition of H_3PO_4 elucidate that the anodic shift of the β-PbO_2 peak with increased H_3PO_4 concentration leads to an overlapping with the oxygen evolution. Therefore the remaining oxidation peak has to be interpreted as the α-PbO_2 peak (Fig. 1, 7×10^{-2} mol/l). This was confirmed by a quantitative determination of the β/α-PbO_2 ratio by X-ray diffraction analysis of the corresponding corrosion layers at different H_3PO_4 concentrations after 80 cycles, illustrated in Fig. 2.

Analogously to the oxidation peaks the PbO_2 reduction peaks show an anodic shift as well accompanied by a decreased peak area and broadening.

The decrease in oxidation and reduction peak area effected by H_3PO_4 is in agreement with the thickness of the corrosion layer shown on the cross section of these electrodes (Fig. 3(c)). Of course the formation of soluble Pb(IV) species would lead to a reduced thickness of the corrosion layer as well and cannot be excluded entirely, however this should cause an increased anodic Pb corrosion peak, which could not be observed. A greater thickness and a higher porosity (cracks) of the corrosion layer at a H_3PO_4 concentration of 10^{-2} mol/l (Fig. 3(b)) is in agreement with the larger peak area observed. That might be explained as a special point between the two contrasting effects of H_3PO_4, the corrosion stimulative effect of a higher Pb^{4+} solubility and the corrosion inhibition effect of the smaller crystal size (will be discussed later) formed in the presence of H_3PO_4.

The results of potentiostatic gas volumetric measurements given in Fig. 4 clearly demonstrate the diminution of the oxygen evolution by phosphoric acid and the

consequently increased oxygen overpotential, as could already be seen by the anodic shift of the oxygen peak in the cyclovoltammogram (Fig. 1, 7×10^{-2} mol/l).

A splitting of the PbO_2 reduction peak in solutions containing phosphoric acid was already detected by Bullock and McClelland [20] and Sternberg *et al.* [30]. At potential scan rates below 10 mV/s we also observed the splitting of the PbO_2 reduction peak in the presence of phosphoric acid. Figure 5 shows the cyclic voltammograms of a lead electrode at the potential scan rate of 0.2 mV/s. In electrolytes containing phosphoric acid up to three reduction peaks partially anodic shifted could be discerned. The anodic shifted peaks suggest the formation of more active PbO_2 (including extremely
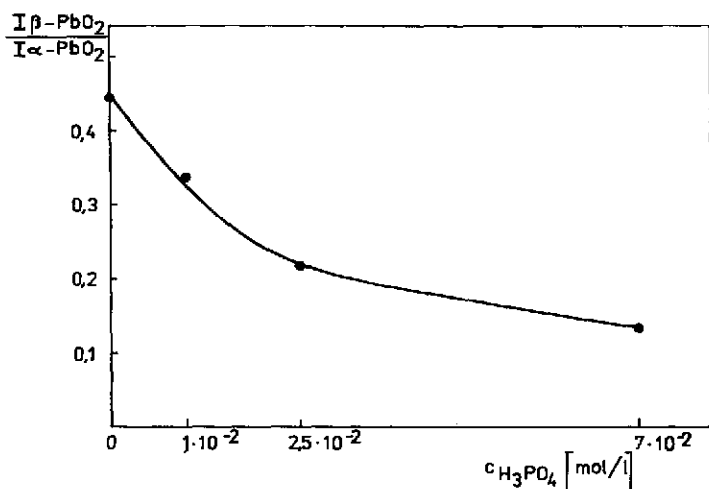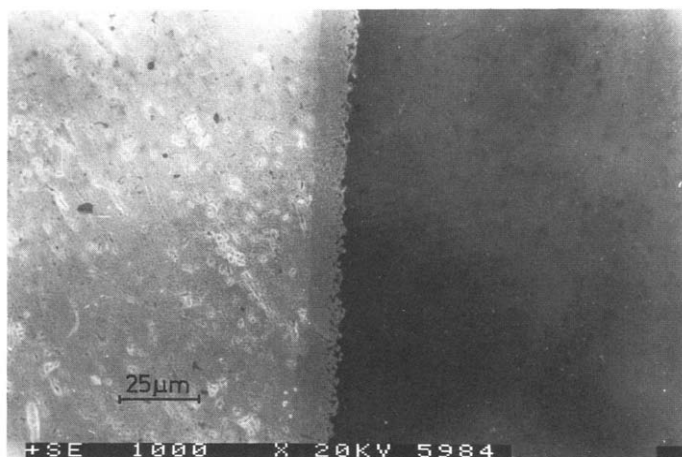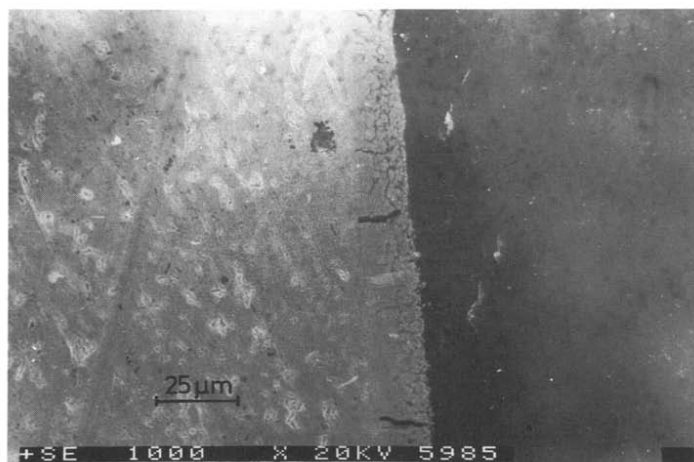

Fig. 2. Ratio of β/α-PbO_2 determined by X-ray analyses on the corrosion layers formed on Pb during 80 cycles in 0.85 M H_2SO_4 containing various amounts of H_3PO_4.

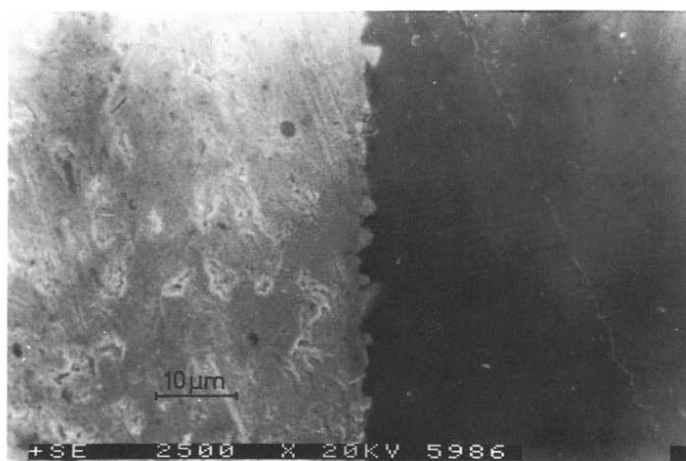(a)

Fig. 3.   *(continued)*

(b)

(c)

Fig. 3. Cross section of the corrosion layer formed on a cycled lead electrode in 0.85 M H_2SO_4 containing various amounts of phosphoric acid: (a) 0 mol/l, (b) 10^{-2} mol/l, (c) 2.5×10^{-2} mol/l; magnification for (c) is 2.5 times higher than for (a) and (b).

fine grained or amorphous PbO_2) or the formation of further compounds. With increasing number of cycles, however, these peaks melt into one peak again.

No comprehensive explanation exists for this cathodic peak splitting. Laitinen and Watkins [25] observed three and more reduction peaks in stripping analyses of multiple PbO_2 layers in nitrate electrolytes that contained H_3PO_4. They are of the opinion that the adsorption of phosphate effects an inhibition of the growth of a PbO_2 layer which can be reduced reversibly. Sternberg et al. [30] assumed that the double peak observed in their experiments represented two electrochemical reactions with respect to the reduction of PbO_2 to $PbSO_4$ in the presence of phosphoric acid. Kinard and Probst [31], however, also observed the splitting into two reduction peaks in sulfuric acid of
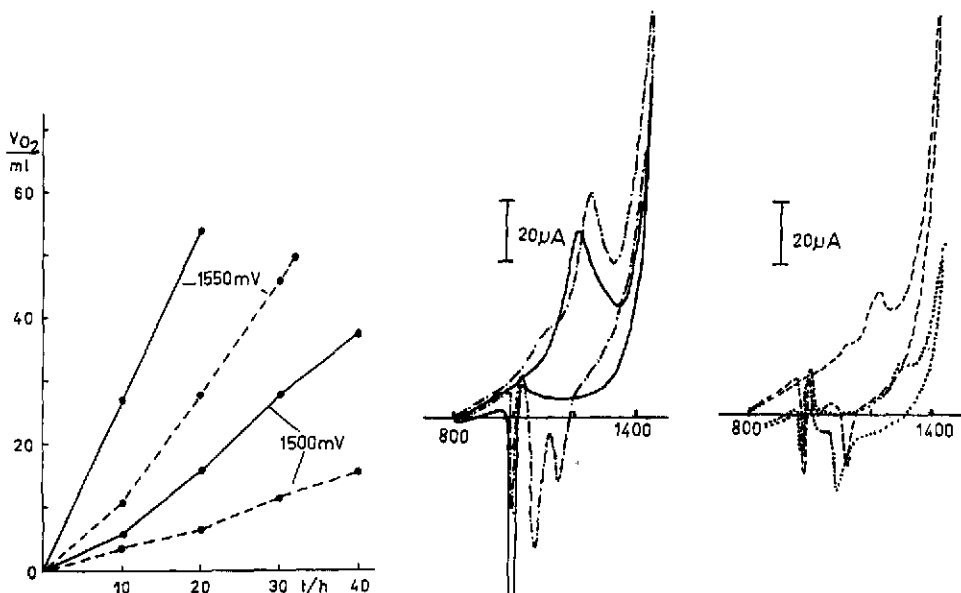
Fig. 4. Oxygen evolution on lead rod electrodes ($A = 10$ cm^2) during anodic polarization in 4.93 M H$_2$SO$_4$. H$_3$PO$_4$: —— 0 mol/l, — — — 2.5 $\times 10^{-2}$ mol/l.

Fig. 5. Cyclovoltammograms of PbO$_2$/PbSO$_4$ electrodes during the 2nd cycle in 0.85 M H$_2$SO$_4$ containing phosphoric acid in the potential range $+800$—$+1450$ mV, $v = 0.2$ mV/s. —— 0 mol/l, — · — · — 10^{-2} mol/l, — — — 2.5$\times 10^{-2}$ mol/l, · · · · · 7$\times 10^{-2}$ mol/l.

low concentration (0.01 M) that was free of phosphoric acid. Carr and Hampson [22] concluded that PbHPO$_4$ might be formed as an adsorbate during the reduction process. By means of X-ray analyses Bullock and McClelland [20] succeeded in proving the existence of Pb$_3$(PO$_4$)$_2$ within the corrosion layer formed at potentials between 1230 and 1275 mV in sulfuric electrolyte containing H$_3$PO$_4$. In our X-ray diffraction measurements we could not detect any lead phosphate compounds.

As shown by scanning electron microscope photos of the electrode surface which have been taken in the discharged state after 80 cycles (Fig. 6), crystallites of PbSO$_4$ formed in the presence of phosphoric acid differ in their shape and dimension (Fig. 6(b)). PbSO$_4$ formed in electrolyte free of phosphoric acid has a relatively uniform floe-like structure (Fig. 6(a)) whereas PbSO$_4$ formed in electrolyte containing H$_3$PO$_4$ has a quite different appearance; comparatively coarse crystals are surrounded by small crystallites. Their crystal shapes are mainly double tetrahedrons. The crystalline layer is very thin and the crystals are placed on an extremely fine grained and almost amorphous layer (Fig. 6(b)). This is in agree with experimental results given in ref. 29. We assume the difference in crystal structure and dimension includes a difference in the overpotential of crystallization. Thus might cause the splitting of the reduction peak, however the formation of lead phosphate compounds should be taken into consideration too.

The results of the local electron microprobe analyses of the electrode surface demonstrated that phosphorus incorporation occurred only in the extremely fine grained region. Since the characteristic lines of phosphorus (P$_{K-\alpha}$ = 2.015 keV), was
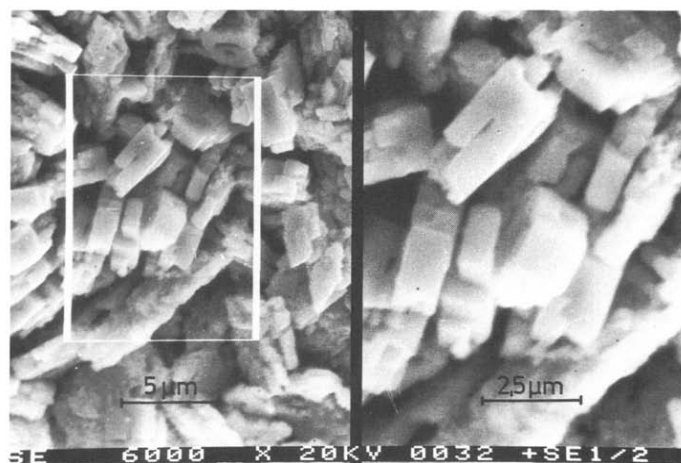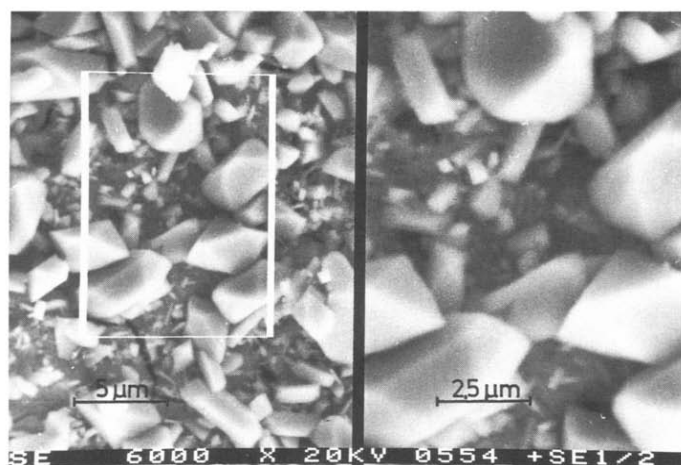
Fig. 6. Influence of H_3PO_4 on particle morphology of $PbSO_4$ at the surface of the discharged PbO_2 electrode after 80 cycles in 0.85 M H_2SO_4: (a) 0 mol/l, (b) 2.5×10^{-2} mol/l.

overlapped by the intense peaks of lead ($Pb_{M-\alpha} = 2.342$ keV) and sulfur ($S_{K-\alpha} = 2.308$ keV) the spectra of difference presented in Fig. 7, curve C was used for phosphorus detection. Curve C was derived from the spectra of the fine grained region (curve A) and the spectra of the coarse grained region (curve B). By analogous comparative measurements on the coarse grained region no phosphorus content was detected. Apparently the big crystals are growing during the reduction phase, however, in the oxidation phase they seem to be oxidized only a little.

Figure 8 illustrates the concentration of phosphorus, sulfur and lead on the electrode surface (area of analysis 80×80 μm^2) after cycling (80 cycles, removed at 1600 mV, quickly washed and dried) in dependence on H_3PO_4 concentration. Surprisingly the detected phosphorus concentration at the electrode surface was almost independent
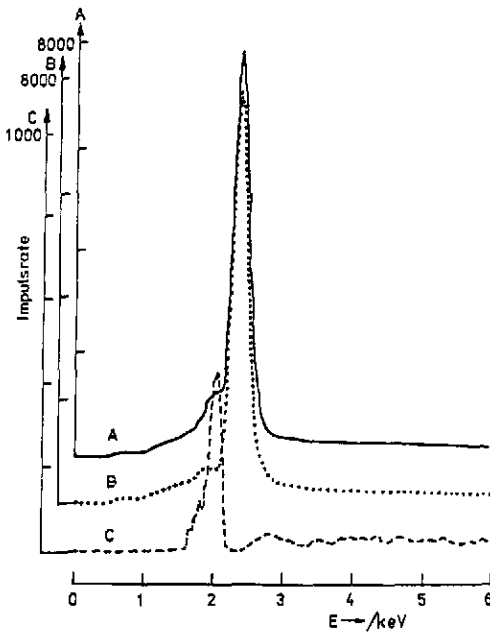
Fig. 7. X-ray emission spectra of the $PbO_2/PbSO_4$ electrode surface obtained by electron microprobe analysis: (A) fine grained region, (B) coarse grained region, (C) difference curve derived from (A) and (B). Characteristic X-ray line of phosphorus 2.015 keV.
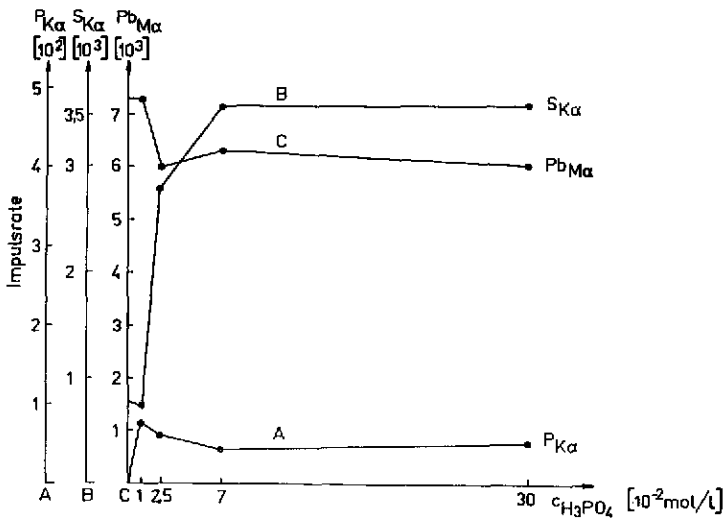

Fig. 8. Electron microprobe analysis of sulfur, lead and phosphorus on an PbO_2 electrode surface (charged state) subjected to 80 cycles in 0.85 M H_2SO_4 containing different amounts of H_3PO_4.

above a threshold of the H_3PO_4 concentration in the electrolyte within the tested range. This suggests that phosphorus is mainly bound at the surface by specific adsorption and not directly incorporated into the $PbO_2/PbSO_4$ structure. Therefore, it might make more sense to give the H_3PO_4 concentration as the molar ratio of PbO_2/H_3PO_4 from the practical point of view. In practical cells this molar ratio is in the range of 20–40 whereas in our case this ratio was in the range of 10^{-5}–10^{-3} in dependence on the cycle for the investigated smooth electrodes.

The sulfur concentration is increased in a step-like manner at phosphoric acid concentrations above 10^{-2} mol/l. This result supports our previous assumption (derived from deep discharge after anodic cycling) that a dense $PbSO_4$ layer of inhibited tendency to oxidation is formed on the electrode surface when the electrolyte contains H_3PO_4 [32]. This dense layer prevents the reduction of the PbO_2 underneath in the cathodic sweep.

What is the origin of the fine grained structure of $PbSO_4$? Hampson and co-workers found a specific anion adsorption on the PbO_2 electrode in sulfate [33] as well as in phosphate electrolytes [22]. A comparison of differential capacitance shows that values of about 2.5 times higher were obtained in sulfate electrolyte.

Differential capacitance of electrodes resulting from our impedance measurements in mixed electrolytes of sulfuric and phosphoric acid are presented in Fig. 9. The decrease of differential capacitance by about 15% in electrolyte that contains H_3PO_4 is effected by adsorption of phosphate ions on the PbO_2 electrode. The phosphate ion adsorption during the formation of PbO_2 cause it to have properties that lead to a decreased reduction peak of the PbO_2 electrode. However, with PbO_2 formed in the absence of H_3PO_4, when the phosphoric acid was added to the electrolyte immediately before cathodic scan, the reduction peak of PbO_2 was almost not influenced as we have shown already in our previous paper [32].

From these results we concluded that phosphoric acid primarily influences the oxidation process and no inhibition of PbO_2 reduction by H_3PO_4 adsorption takes place which could attribute to a decrease of the reduction peak.

Alteration in nucleation and nuclei growth processes during lead sulfate oxidation were studied by potential step experiments. The potential of the electrode was jumped
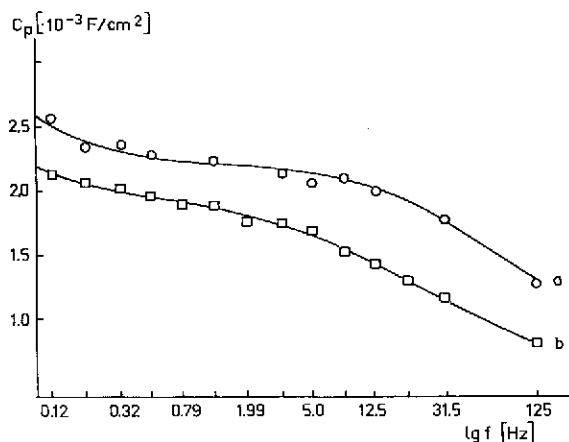

Fig. 9. Differential capacitance of a PbO_2 obtained by impedance measurements in dependence on the frequency and the amount of phosphoric acid added: (a) 0 mol/l, (b) 4×10^{-2} mol/l.

between $+870$ and 1400 mV for 60 s, respectively (anodic = cathodic overpotential = 265 mV). The dependence of the anodic oxidation current on time after 100 repetitions is shown in Fig. 10. The initial current maximum is caused by the continuous formation of Pb^{4+} ions and the formation of an oxygen adsorption layer as well as the current resulting from charging the double layer capacitance. Due to the continuous formation of Pb^{4+} ions, supersaturation is attained and overpotential increases. The constant value of applied potential leads to a decrease of the current and the plot of current versus time reaches the first minimum. Within this time range PbO_2 nucleation starts. When the current increases again a further growth of nuclei already formed occurs simultaneously with further nucleation.

Increasing the concentration of H_3PO_4 effects a prolongation of the induction period. Due to the adsorption of phosphate ions $PbSO_4$ oxidation is inhibited. On the other hand solubility of Pb^{4+} ions is increased by phosphoric acid [27]. Each of these facts results in a prolongation of the induction period. Later an elevated solubility of Pb^{4+} ions causes an increase in nucleation, i.e., a greater number of Pb^{4+} ions causes an increase in nucleation which leads to the formation of an extremely fine grained layer.

We have considered the period between t_0 (t_0 = end of induction period) and t_{max} (t_{max} = time of the first current maximum). Within this period the plotted current over $(t-t_0)^3$ is represented by a straight line for the electrode in pure sulfuric acid while in the presence of H_3PO_4 the analogous current has to be plotted versus $(t-t_0)^2$ for linear dependence. These two linear functions indicate an alteration in the PbO_2 growth mechanism caused by the adsorption of phosphate ions [29, 34, 35]. In an electrolyte free of phosphoric acid a three dimensional growth with progressive nucleation will occur, while by adding H_3PO_4 to the electrolyte the mechanism changes to a two dimensional growth with instantaneous nucleation. Phosphoric acid causes the initial concentration of Pb^{4+} ions to increase. This results in a greater number of nuclei and due to adsorption nuclei growth can only be realized by two-dimensional growth. Thus a PbO_2 morphology is produced which forms an extremely fine grained $PbSO_4$ structure during discharge and leads to a rapid covering of surface.
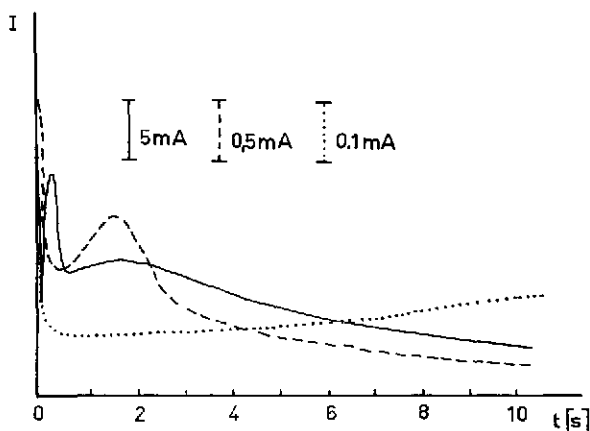

Fig. 10. Current time response of $PbSO_4$ oxidation on a smooth $PbSO_4/PbO_2$ electrode during the 100th anodic potential step between $+870$ and 1400 mV in H_2SO_4 containing H_3PO_4: —— 0 mol/l, – – – 2.5×10^{-2} mol/l, $\cdots\cdots$ 7×10^{-2} mol/l.

Conclusions

Addition of phosphoric acid to the sulfuric acid electrolyte prevents the early passivation of PbO_2 electrodes which usually occurs when using grids free of antimony at cyclic deep discharge. The formation of sulfates throughout the corrosion layer during discharge is one of the possible reasons for passivation. A different explanation was given in refs. 36 and 37. In the charging phase the corrosion layer will not be reoxidized completely to PbO_2. Thus an accumulation of $PbSO_4$ takes place. Adsorption of phosphate ions brings about a change in nucleation and nuclei growth of PbO_2 from a three dimensional growth mechanism with progressive nucleation to a two dimensional growth mechanism with instantaneous nucleation. When PbO_2 formed in this manner is discharged a $PbSO_4$ of extremely fine grained and very densely packed structure is produced. In this way the PbO_2 is covered rapidly and protected against discharge. Consequently sulfate formation is restricted to the outer layer which can again be transformed almost completely into PbO_2 during the subsequent charging phase.

Unfortunately the effect of phosphoric acid is not limited to the corrosion layer only; it influences the active material of the positive electrode in the same manner. Thus hardness and stability of the active material are increased but on the other hand, however, the A h capacity supplied by the cell is diminished by about 10–15% [32].

References

1 C. Brault, *US Patent 625 287* (1899).
2 E. A. Sperry, *US Patent 660 228* (1900).
3 F. D. Cheney, *US Patent 1 385 305* (1921).
4 M. Kugel, *Ger. Patent 480 149* (1928).
5 K. Neumann, *Fr. Patent 690 409* (1930).
6 H. R. Harner, M. F. Chubb, *US Patent 2 035 315* (1935).
7 D. Evers, *US Patent 3 011 077* (1961).
8 E. A. Willihnganz, *Fr. Patent 1 517 629* (1968).
9 S. Tudor, A. Weisstuch and S. H. Davang, *US Patent 3 344 969* (1969).
10 K. Yonetsu, *Jap. Patent 48-5175* (1973).
11 K. Arndt, *ETZ, 56* (1935) 122.
12 C. Drotschmann, *Bleiakkumulatoren*, Verlag Chemie, GmBH, Weinheim, 1951.
13 E. J. Ritchie, Pastes and grids for lead–acid battery, Eagle–Pitcher Industries, *Progress Report No. 2, Combined ILZRO Research Contracts LE-82 and LE-84*, Dec. 1967.
14 M. H. Littele, *US Patent 3 530 002* (1970).
15 R. F. Amlie, *US Patent 3 556 860* (1971).
16 O. Jache, *US Patent 3 756 952* (1973).
17 R. F. Amlie, N. M. Qureshi and E. Y. Weismann, *Proc. 25th Power Source Symp., Atlantic City, May, 1972,* p. 67.
18 R. F. Amlie, E. Y. Weismann, C. K. Morehouse and N. M. Qureshi, *J. Electrochem. Soc., 119* (1972) 568.
19 S. Tudor, A. Weisstuch and S. H. Darang, *Electrochem. Technol., 3* (1965) 90; *4* (1966) 406; *5* (1967) 21.
20 K. R. Bullock and D. H. McClelland, *J. Electrochem. Soc., 124* (1977) 1478; *126* (1979) 360; *126* (1979) 1848.
21 B. K. Mahato, *J. Electrochem. Soc., 126* (1979) 366.
22 J. P. Carr and N. A. Hampson, *J. Electrochem. Soc., 28* (1970) 65.

23 H. Bode and E. Voss, *Electrochim. Acta, 6* (1962) 11.
24 V. F. Huber and M. S. A. El-Meligy, *Z. Anorg. Allg. Chem., 367* (1969) 154.
25 H. A. Laitinen and N. H. Watkins, *Anal. Chem., 47* (1975) 1352.
26 M. Fleischmann, J. R. Mansfield , H. R. Thirsk, H. G. E. Wilson and L. Wynne Jones, *Electrochim. Acta, 12* (1967) 967.
27 R. F. Amlie and T. A. Berger, *J. Electroanal. Chem., 36* (1972) 427.
28 E. Voss, *J. Power Sources, 24* (1988) 171.
29 G. A. Morris, P. J. Mitchell, N. A. Hampson and J. I. Dyson, in T. Keily and B. W. Baxter (eds.), *Power Sources 12,* Int. Power Sources Symp. Comm., Leatherhead, 1989, Academic Press, New York, 1989, p. 61.
30 S. Sternberg, A. Mateeson, V. Branzoni and L. Apateanu, *Electrochim. Acta, 32* (1987) 349.
31 J. T. Kinard and R. C. Probst, *Anal. Chem., 46* (1974) 1106.
32 J. Garche, H. Döring and K. Wiesener, *J. Power Sources, 33* (1991) 213.
33 J. P. Carr, N. A. Hampson and R. Taylor, *J. Electroanal. Chem., 27* (1970) 201.
34 A. C. Ramamurthy and T. Kuwana, *J. Electrochem. Soc., 135* (1982) 243.
35 H. R. Thirsk and J. A. Harrison, *A Guide to the Study of Electrode Kinetics,* Academic Press, London, 1972.
36 A. Winsel, E. Voss and U. Hullmeine, *J. Power Sources, 30* (1990) 231.
37 E. Meissner and E. Voss, *J. Power Source, 33* (1991) 231.